Characteristics of the JRA-55 and ERA-Interim Datasets by Using the Three-Dimensional Normal Mode Energetics

Akio Yamagami[1] and H. L. Tanaka[2]
[1]*Graduate School of Life and Environmental Sciences, University of Tsukuba, Tsukuba, Japan*
[2]*Center for Computational Sciences, University of Tsukuba, Tsukuba, Japan*

Abstract

In this study, we conducted an energetics analysis of the atmospheric general circulation for up-to-date reanalyses, JRA-55 and ERA-Interim, and compared the result with that of the old reanalysis, JRA-25. Since three-dimensional normal mode functions are used, we can separate the energy spectrum into Rossby and gravity components.

According to the comparison between JRA-55 and ERA-Interim, it is found that the characteristics of the energy spectrum and the energy interaction are quite similar in zonal wavenumber and vertical mode domains. However, kinetic energy of Rossby modes for JRA-55 is larger than that for ERA-Interim in all wavenumbers. On the other hand, kinetic energy of gravity modes for JRA-55 is smaller than that for ERA-Interim in small wavenumbers. Therefore, one of the features of JRA-55 is that the wind and geopotential fields are close to the geostrophic balance.

According to the comparison among JRA-55, ERA-Interim and JRA-25, the imbalance for JRA-55 at zonal wavenumbers 10 to 25 is similar to ERA-Interim and is smaller than that for JRA-25. It is also found that the interactions of available potential energy in the zonal wavenumber domain for JRA-55 is comparable to that for ERA-Interim and is larger than that for JRA-25.

(**Citation**: Yamagami, A., and H. L. Tanaka, 2016: Characteristics of the JRA-55 and ERA-Interim datasets by using the three-dimensional normal mode energetics. *SOLA*, **12**, 27−31, doi: 10.2151/sola.2016-006.)

1. Introduction

Energetics analysis is a powerful tool to diagnose the atmospheric general circulation. Lorenz (1955) introduced available potential energy and conducted the energetics analysis of the atmosphere for the first time. He calculated the energy of zonal and eddy components and energy conversions of zonal-eddy and eddy-eddy interactions of kinetic and available potential energies. The energy flow is called Lorenz cycle. Saltzman (1957, 1970) expanded the Lorenz cycle of atmospheric energy in wave number space, and revealed details of zonal-wave and wave-wave interactions. The energy flow is called Saltzman cycle. Furthermore, Bore and Shepherd (1983) expanded the energetics to two-dimensional energy distributions by using spherical harmonic functions. They showed that the energy distributions of the atmospheric general circulation are functions of not only zonal scales but also meridional scales.

Tanaka (1985) developed three-dimensional (3D) normal mode energetics using 3D normal mode functions. He evaluated the energy of the atmospheric general circulation decomposed into Rossby and gravity components and showed the energy spectrum of both components as functions of zonal wavenumbers, meridional modes and vertical modes, respectively. It is known that the zonal energy spectrum obeys the −3 power law which shifts to the −5/3 power law in higher zonal wavenumbers. Recently, the shift of the energy slopes was explained by Terasaki et al. (2011) as the change of dominant modes from Rossby to gravity modes.

Corresponding author: Hiroshi L. Tanaka, University of Tsukuba, 1-1-1 Tennodai, Tsukuba 305-8577, Japan. E-mail: tanaka@ccs.tsukuba.ac.jp.

The results of the energetics analysis depend on the different reanalysis datasets. For example, Watarai and Tanaka (2007) showed some differences between JRA-25, ERA-40 and NCEP reanalyses by using Lorenz's and Saltzman's energy cycles. Tanaka and Kimura (1996) also compared the multiple reanalysis datasets using the 3D normal mode energetics. Likewise, Žagar et al. (2009a, b) applied the 3D normal mode energetics to four different analyses and compared energy levels of gravity modes. With regard to model output, Terasaki et al. (2009) investigated the details of the kinetic energy spectrum of Non-hydrostatic Icosahedral Atmospheric Model (NICAM) for different resolutions by using Fourier analysis, and they showed that the highest resolution model can exhibit the shift of the energy slopes from the -3 power to -5/3 power laws.

The Japanese 55-year reanalysis (JRA-55; Kobayashi et al. 2015) is an up-to-date reanalysis dataset produced by Japan Meteorological Agency (JMA). One of the important features compared to the previous datasets is the change of the data assimilation method from 3D-Var to 4D-Var. ERA-Interim (Dee et al. 2011) is a recent reanalysis dataset produced by European Centre for Medium-Range Weather Forecasts (ECMWF), which is also based on the 4D-Var data assimilation system.

The purpose of this study is (1) to conduct the 3D normal mode energetics analysis using the latest datasets, (2) to investigate the differences among those reanalyses especially for gravity modes and (3) to compare the results with that of the previous reanalysis by JRA-25 (Onogi et al. 2005). In Section 2, methodology and datasets used in this study are described. The results of the energetics analysis are presented in Section3, and the concluding remarks are summarized in Section 4.

2. Data and methodology

In this study, we conducted 3D normal mode energetics analysis that was developed by Tanaka (1985). In this analysis scheme Hough harmonics are used for the horizontal expansion and vertical structure functions for the vertical expansion. In calculation of the vertical structure functions, we used Galerkin's method (Kasahara and Puri 1981) with a fixed value of static stability parameter (γ = 30K) for mean surface temperature (T_s = 300K) to compare different reanalysis datasets using a common expansion basis function. Due to the application of Hough functions, we can separate atmospheric variables into 3 parts: Rossby (rotational) mode, westward gravity mode and eastward gravity mode (Kasahara 1976; 1977). The 3D spectral model for primitive equations expanded in the 3D normal mode functions may be written as follows:

$$\frac{dw_i}{d\tau} + i\sigma_i w_i = -i\sum_j \sum_k r_{ijk} w_j w_k + f_i, \tag{1}$$

where w_i are the expansion coefficients, τ is dimensionless time scaled by the angular speed of Earth's rotation, σ_i are eigenfrequencies of the Laplace's tidal equation, r_{ijk} are interaction coefficients for nonlinear terms, and f_i are expansion coefficients of external forcing of viscosity and diabatic heating rate. The subscripts i, j and k represent different sets of 3D wavenumbers (nlm), where n, l, and m denote zonal, meridional and vertical wavenumbers.

Total energy of each mode (E_{nlm}) is expressed by the expan-

sion coefficient as follows:

$$E_{nlm} = \frac{1}{2} p_s h_m |w_{nlm}|^2, \quad (n > 0), \tag{2}$$

where p_s and h_m denote surface pressure (1013 hPa) and equivalent height for the vertical mode m. The energy spectrum for $n = 0$ is defined by the half value of Eq. (2).

The energy balance equation written in the spectral form is obtained by differentiating Eq. (2) with respect to time and substitute Eq. (1):

$$\frac{dE_{nlm}}{dt} = B_{nlm} + C_{nlm} + D_{nlm}, \tag{3}$$

where terms B_{nlm} and C_{nlm} represent energy interactions associated with kinetic energy and available potential energy, respectively. The summation of these energy interaction terms must be zero when all modes are summed. However, the actual summation is not zero due to numerical error. Therefore we modify these values by adding the residual to the zonal component. The term D_{nlm} represents the sum of energy generation by the differential heating and the energy dissipation by the diabatic processes.

The data used in this study are two latest reanalyses: JRA-55 and ERA-Interim, and one previous reanalysis: JRA-25. These datasets contain horizontal wind (u, v), geopotential ϕ, temperature T, and vertical p-velocity ω, defined at every grid point of 1.25° longitude by 1.25° latitude at 37 pressure levels from 1000 to 1.0 hPa for JRA-55 and ERA-Interim and 23 pressure levels from 1000 to 0.4 hPa for JRA-25. In order to expand in vertical direction, these data are interpolated from those pressure levels to 60 Gaussian vertical levels by cubic spline method. We calculate the energy spectrum and energy interactions by using four times daily (00, 06, 12 and 18 UTC) data for each reanalysis, and average for wintertime (December, January and February) from 1979/80 to 2009/10. Because we are interested in the characteristics of the energy for the large-scale atmospheric circulation, the truncations of zonal wavenumbers and meridional modes are chosen as n = 0−50, l_R = 1−26 and $l_{EG} = l_{WG}$ = 1−12. The truncation of the vertical mode is chosen as m = 0−25 for JRA-55 and ERA-Interim and as m = 0−22 for JRA-25 due to the different numbers of the vertical levels.

3. Results

Figure 1 shows total energy spectra of Rossby and gravity modes for each reanalysis in the zonal wavenumber domain. The energy spectrum of Rossby mode obeys the −3 power law and that of gravity mode obeys the −5/3 power law at higher wavenumbers ($n \geq 6$). The magnitude of energy for Rossby and gravity modes becomes comparable in higher wavenumbers.

Figure 2 shows kinetic and available potential energy spectra in the vertical wavenumber domain. Here, the vertical wavenumber is calculated as a wavenumber (μ_m) in a log-pressure vertical coordinate as in Eq. (8) of Terasaki and Tanaka (2007) as follows:

$$\mu_m = \sqrt{\left| \frac{1}{4} - \frac{R\gamma}{gh_m} \right|}$$

where R is the gas constant of dry air and g is Earth gravity acceleration. As the barotropic mode (m = 0) does not have a node and cannot define the vertical wavenumber, the energy spectrum of barotropic mode is plotted at the left corner by different symbols for the sake of convenience. The energy spectrum in the vertical wavenumber domain has two energy peaks, i.e., barotropic and m = 4 of the baroclinic mode (the equivalent height corresponds to ~250 m). The kinetic energy is dominant in the barotropic component and the available potential energy is dominant at m = 4 of the baroclinic component. The kinetic energy spectrum follows the −3 power law from the vertical wavenumber 2 to 10, which agrees with the vertical energy spectrum by Terasaki (2009).

The kinetic energy spectrum becomes less steep in higher wavenumbers, and the energy of Rossby and gravity modes becomes nearly the same magnitude around this scale (Supplement 1). According to the results, it is found that the energy slope in the vertical wavenumber domain has a similar relation as the zonal wavenumber spectrum, i.e., the dominant mode changes from Rossby mode to gravity mode. However, vertical structure functions used in this study are constructed by Galerkin's method in contrast to the analytical method in Terasaki (2009). It is known that vertical structure functions constructed by the numerical method are quite different from that constructed by the analytical method at higher order vertical modes due to the aliasing. There-

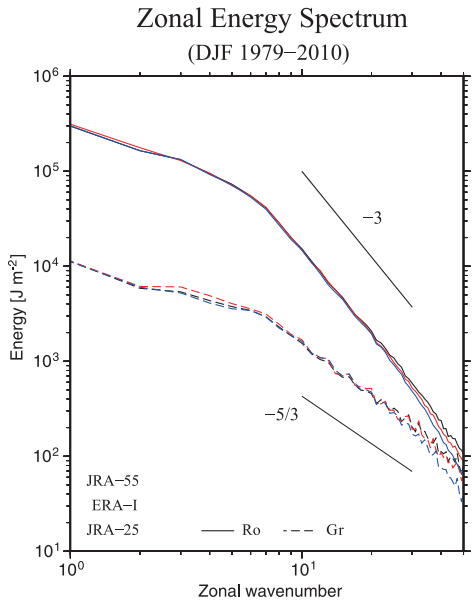

Fig. 1. Total energy spectra of the Rossby (solid line) and gravity (broken line) modes in zonal wavenumber domain. Black, red and blue colors represent JRA-55, ERA-Interim and JRA-25.

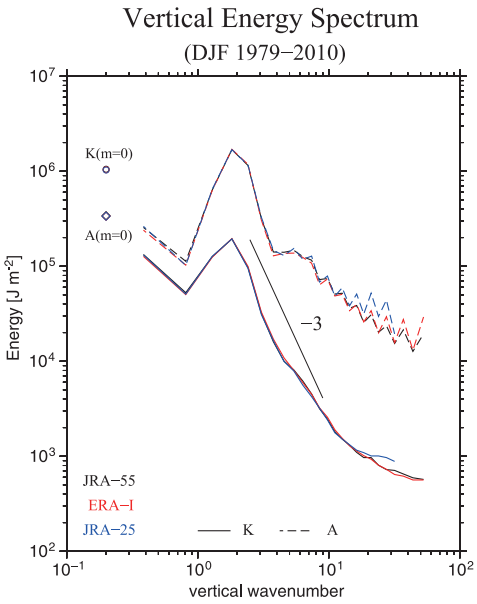

Fig. 2. Distribution of kinetic (solid line) and available potential energy (broken line) spectra in the vertical wavenumber domain. The circle and rhombus symbols are barotropic components of kinetic and available potential energies, respectively. Each color represents the different reanalysis as in Fig. 1.

fore, it needs more careful investigation for higher order vertical modes.

Figure 3 shows differences of kinetic energy between (a) JRA-55 and JRA-25, and (b) JRA-55 and ERA-Interim in zonal wavenumber domain. Because the abscissa is logarithmic axis, the energy difference of zonal component (n = 0) is plotted at left corner by different symbols for the sake of convenience. The most remarkable characteristic in Fig. 3 is that the kinetic energy of Rossby modes for JRA-55 is larger than that for JRA-25 and ERA-Interim in all wavenumbers. With respect to gravity modes, the kinetic energy for JRA-55 is smaller than that for JRA-25 in n = 10−25. Since the same characteristic is also shown for the available potential energy of gravity modes in this range (not shown), it is found that JRA-25 contains artificial gravity waves. In contrast, the kinetic energy of gravity mode for JRA-55 is larger than that for JRA-25 in n = 3−9 and $n \geq 25$. The energy of gravity modes for ERA-Interim is larger than that for JRA-55 in n = 0−10, and the energy spectrum of gravity modes for JRA-55 is almost comparable to that for ERA-Interim in smaller scale ($n > 10$). This relation of the difference for each scale can be seen in available potential energy spectrum of gravity modes. According to Figs. 1 and 2, the difference of the total energy for each reanalysis is quite small, and characteristics of the spectral peak and slope are quite similar. However, it is found that the general circulation for JRA-55 is highly balanced between wind and geopotential compare to other reanalysis datasets.

According to the energy difference of zonal component, the energy for JRA-55 is larger than that for JRA-25 in both Rossby and gravity modes. The energy of Rossby mode for JRA-55 is also larger than that for ERA-Interim, while the energy of gravity mode for JRA-55 is smaller than that for ERA-Interim. Therefore, the result of larger gravity mode energy for n = 0 suggests that the Hadley circulation in the tropics is strong for ERA-Interim, JRA-55 and JRA-25 in tern. Likewise, the result of larger Rossby mode energy for n = 0 suggests that the mid-latitude jet stream is strongest for JRA-55.

Figure 4 shows total energy spectra of Kelvin and mixed Rossby-gravity (MRG) modes in the zonal wavenumber domain (Fig. 4a) and in the vertical wavenumber domain (Fig. 4b). These modes are most important in the tropics. In Fig. 4a, the energy spectrum of MRG mode follows the −3 power law in the synoptic scale with the energy peak at n = 6, while the energy spectrum of Kelvin mode almost follows the −5/3 power law in all wavenumbers with the peak at n = 1. In Fig. 4b the energy of barotropic mode is plotted at the left corner of the graph for Kelvin and MRG as in Fig. 2. According to the result, the energy spectrum of MRG mode shows the peaks at m = 0 and 4, and the spectrum follows the −3 power law in the higher order vertical modes which was not seen in Tanaka (1985). The energy spectrum of Kelvin mode shows a single peak at m = 4 with lower energy level for m = 0.

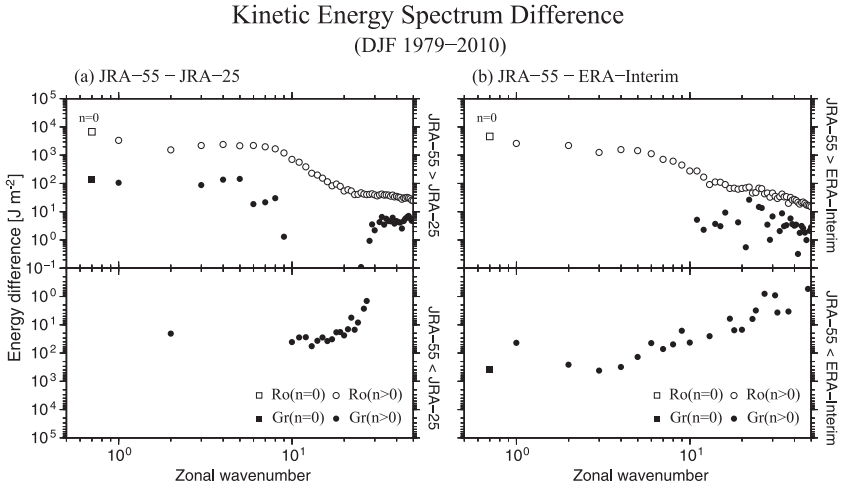

Fig. 3. Difference of kinetic energy spectra in the zonal wavenumber domain for (a) JRA-55 subtracted by JRA-25 and for (b) JRA-55 subtracted by ERA-Interim. The positive values are plotted at the upper panel of the figure and the negative values are plotted at the lower panel of the figure. The white and black symbols represent Rossby and gravity modes, respectively. Zonal component (n = 0) is plotted at left corner by square symbols for the sake of convenience.

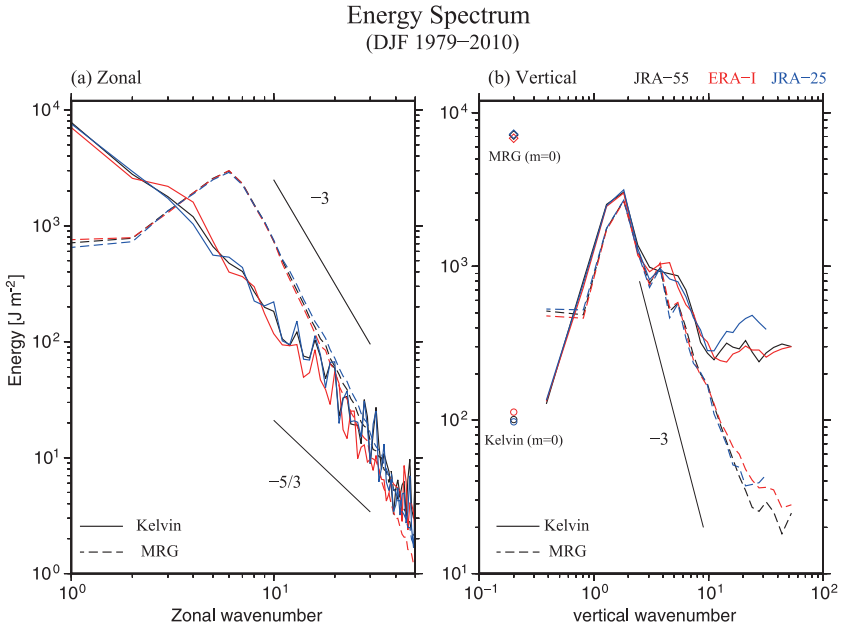

Fig. 4. Distribution of energy spectra of Kelvin (solid line) and Mixed Rossby-gravity (broken line) modes in the zonal wavenumber (left) and in the vertical wavenumber (right) domains. The circle and rhombus symbols in right panel are barotropic components of Kelvin and MRG mode energies, respectively. Each color represents the different reanalysis as in Fig. 1.

The energy levels are higher than that of MRG at the higher order vertical modes.

The comparison of each reanalysis indicates almost similar energy spectrum for Kelvin and MRG modes. However, the difference of energy spectrum can be seen in the larger vertical wavenumbers.

Figure 5 shows the kinetic and available potential energy interactions for each reanalysis in the zonal wavenumber domain (Fig. 5a) and in the vertical mode domain (Fig. 5b). According to the results for Fig. 5a, available potential interactions C show large positive values at n = 3 and 6, while kinetic energy interactions B shows large negative values at n = 2 and 6. The different signs between B and C indicate the baroclinic energy conversion from available potential energy to kinetic energy in the synoptic-scale disturbances (n = 5−8). According to the results for Fig. 5b in the vertical mode domain, kinetic energy interactions B show negative values at m = 3−5 and a large positive value at m = 0, indicating energy interactions from baroclinic to barotropic components. The energy interactions C show positive values for m = 4 and 5 and negative values for higher order vertical modes, indicating an energy cascade from lower to higher vertical modes. The comparison for each reanalysis suggests that the difference in energy interactions is negligibly small except for smaller interactions for C in the zonal wavenumbers for JRA-25.

4. Conclusion

In this study, we conducted the energetics analysis of atmospheric general circulation in winter for JRA-55, ERA-Interim and JRA-25 reanalyses by using 3D normal mode expansion. JRA-55 and ERA-Interim are the latest reanalyses, which are improved in resolution, data assimilation method, chemical processes, among others. From the results of the analysis, the energy peaks and the energy slopes for different reanalysis agree with each other. The energy interactions of kinetic and available potential energies also showed almost same features for each reanalysis.

However, the comparison of the kinetic energy spectrum among the reanalysis datasets showed that JRA-55 has the largest energy of Rossby mode in all scales. On the other hand, the kinetic energy of gravity mode for JRA-55 in planetary to synoptic scale is smaller than that for ERA-Interim. In the small scale (n > 10), the kinetic energy of gravity mode is comparable for these reanalyses. Therefore, as one of the features of JRA-55, the relation between wind and geopotential is closer to the geostrophic balance than that of other two datasets, whereas the small-scale motions associated with the gravity modes are comparable to that for ERA-Interim. In addition, JRA-55 has larger zonal kinetic energy of Rossby modes compared to other two reanalyses indicating a strong jet stream in mid-latitudes. According to the result of the energy interactions, the strength of baroclinic conversion associated with synoptic scale disturbance is almost same as for ERA-Interim.

According to the comparison for JRA-55 and JRA-25, JRA-25 has larger energy of gravity modes in the intermedium scale (10 < n < 25). However, owing to the finer resolution and advanced data assimilation method, the gravity mode energy for JRA-55 became larger than that for JRA-25 for the small scale (25 < n). Thus, the excessive gravity mode energy for JRA-25 might come from the artificial imbalance in 3D-Var. Furthermore, it is found that the zonal energy of Rossby and gravity modes is larger in JRA-55 than JRA-25 suggesting the stronger jet stream in mid-latitude and Hadley circulation in the tropics. According to the result of the energy interactions, the strength of baroclinic conversion for JRA-55 is stronger than for JRA-25.

In this study, we focus the energetics in winter climate from 1979 to 2010. However, the difference in the energetics might be much larger in a shorter time scale for different reanalyses. It is desirable to compare the energy cycle focusing on the extreme event, for example, the prominent Arctic Oscillation negative in 2009/10 and strong Madden-Julian Oscillation event in March 2015.

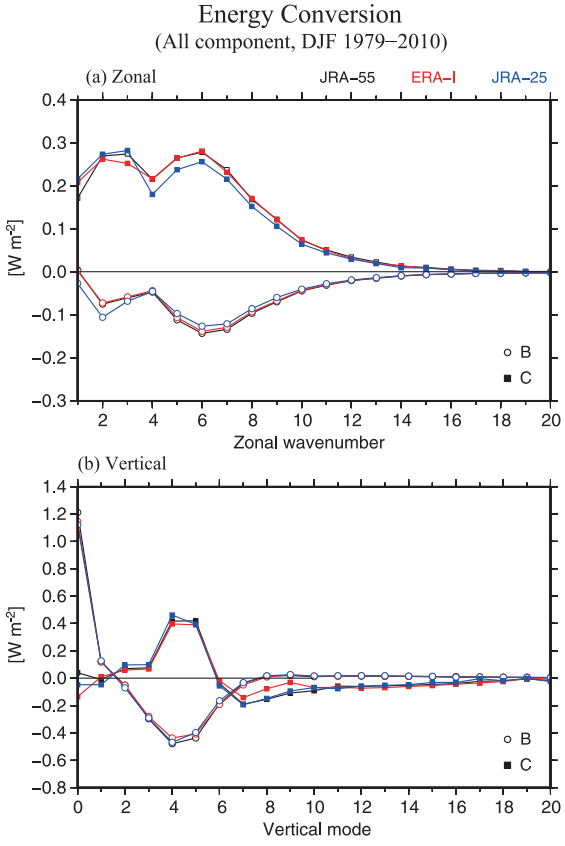

Fig. 5. Distribution of kinetic energy interaction (circle) and available potential energy interaction (square) in the zonal wavenumber domain (upper) and in the vertical mode domain (lower). Each color represents the different reanalysis as in Fig. 1.

Acknowledgements

The authors are grateful to JMA, Central Research Institute of Electric Power Industry (CRIEPI) and ECMWF for providing reanalysis datasets. All figures were drawn by the Generic Mapping Tools (GMT) graphics.

Edited by: H. Mukougawa

Supplement

The figure in Supplement 1 shows the distribution of the kinetic energy spectrum of Rossby (solid line) and gravity (broken line) modes in the vertical wavenumber domain. The circle and rhombus symbols are barotropic components of Rossby and gravity mode energies, respectively. Each color represents the different reanalysis as in Fig. 1.

References

Bore, G. J., and T. G. Shepherd 1983: Large-scale two-dimensional turbulence in the atmosphere. *J. Atmos. Sci.*, **40**, 168−184.

Dee, D. P., S. M. Uppala, A. J. Simmons, P. Berrisford, P. Poli, S. Kobayashi, U. Andrae, M. A. Balmaseda, G. Balsamo, P. Bauer, P. Bechtold, A. C. M. Beljaars, L. van de Berg, J. Bidlot, N. Bormann, C. Delsol, R. Dragani, M. Fuentes, A. J. Geer, L. Haimberger, S. B. Healy, H. Hersbach, E. V. Hólm, L. Isaksen, P. Kållberg, M. Köhler, M. Matricardi, A.

P. McNally, B.M. Monge-Sanz, J.-J. Morcrette, B.-K. Park, C. Peubey, P. de Rosnay, C. Tavolato, J.-N. Thépaut, and F. Vitart, 2011: The ERA-Interim reanalysis: Configuration and performance of the data assimilation system. *Quart. J. Roy. Meteor. Soc.*, **137**, 553−597.

Kobayashi, S., Y. Ota, Y. Harada, A. Ebita, M. Moriya, H. Onoda, K. Onogi, H. Kamahori, C. Kobayashi, H. Endo, K. Miyaoka, and K. Takahashi, 2015: The JRA-55 reanalysis: General specifications and basic characteristics. *J. Meteor. Soc. Japan*, **93**, 5−48.

Kasahara, A., 1976: Normal modes of ultralong waves in the atmosphere. *Mon. Wea. Rev.*, **104**, 669−690.

Kasahara, A., 1977: Numerical integration of the global barotropic primitive equations with Hough harmonic expansions. *J. Atmos. Sci.*, **34**, 687−701.

Kasahara, A., and K. Puri, 1981: Spectral representation of three-dimensional global data by expansion by normal mode functions. *Mon. Wea. Rev.*, **109**, 37−51.

Lorenz, E. N., 1955: Available potential energy and the maintenance of the general circulation. *Tellus*, **7**, 157−167.

Onogi, K., J. Tsutsui, H. Koide, M. Sakamoto, S. Kobayashi, H. Hatsushika, T. Matsumoto, N. Yamazaki, H. Kamahori, K. Takahashi, S. Kadokura, K. Wada, K. Kato, R. Oyama, T. Ose, N. Mannoji, and R. Taira, 2007: The JRA-25 Reanalysis. *J. Meteor. Soc. Japan*, **85**, 369−432.

Saltzman, B., 1957: Equations governing the energetics of the larger scales of atmospheric turbulence in the domain of wavenumber. *J. Meteor.*, **14**, 513−523.

Saltzman, B., 1970: Large-scale atmospheric energetics in the wave-number domain. *Rev. Geophys.*, **8**, 289−302.

Tanaka, H. L., 1985: Global energetics analysis by expansion into three dimensional normal mode functions during the FGGE winter. *J. Meteor. Soc. Japan*, **63**, 180−200.

Tanaka, H., and K. Kimura, 1996: Normal-mode energetics analysis and the intercomparison for the recent ECMWF, NMC, and JMA global analyses. *J. Meteor. Soc. Japan*, **74**, 525−538.

Terasaki, K., 2009: Spectral Energetics Analysis of the General Circulation of the Atmosphere Using the Analytical Vertical Structure Functions. *Doctoral Dissertation for Life and Environmental Science*, University of Tsukuba, pp. 82.

Terasaki, K., and H. L. Tanaka, 2007: An analysis of the 3D atmospheric energy spectra and interactions using analytical vertical structure functions and two reanalyses. *J. Meteor. Soc. Japan*, **85**, 785−796.

Terasaki, K., H. L. Tanaka, and M. Satoh, 2009: Characteristics of the kinetic energy spectrum of NICAM model atmosphere. *SOLA*, **5**, 180−183.

Terasaki, K., H. Tanaka, and N. Zagar, 2011: Energy spectra of Rossby and gravity waves. *SOLA*, **7**, 45−48.

Watarai, Y., and H. Tanaka, 2007: Characteristics of the JRA-25 dataset from the viewpoint of global energetics. *SOLA*, **3**, 9−12.

Žagar, N., J. Tribbia, J. L. Anderson, and K. Rader, 2009a: Uncertainties of estimates of inertia-gravity energy in the tmosphere. Part I: Intercomparison of four analysis systems. *Mon. Wea. Rev.*, **137**, 3858−3873.

Žagar, N., J. Tribbia, J. L. Anderson, and K. Rader, 2009b: Uncertainties of estimates of inertia–gravity energy in the atmosphere. Part II: Large-scale equatorial waves. *Mon. Wea. Rev.*, **137**, 3878−3857.

Manuscript received 5 November 2015, *accepted 5 January 2016*
SOLA: *https://www.jstage.jst.go.jp/browse/sola/*